First results from recent JET experiments in Hydrogen and Hydrogen-Deuterium plasmas

I. Nunes[1], S. Brezinsek[2] , J. Buchanan[3], K. Cave-Ayland[3], C.D. Challis[3], I. Carvalho[1], E.G. Delabie[4], D. van Eester[5], M. Faitsch[6], J.M. Fontdecaba[3], L. Garzotti[3], M. Groth[7], J. Hillesheim[3], J. Hobirk[6], A. Hubbard[8], A. Huber[6], E. Joffrin[9], Y. Kazakov[5], D. King[3], A. Krasilnikov[10], K. Krieger[6], A.B. Kukushkin[10], E. Lerche[3], E. De La Luna[11], C. Maggi[3], P. Mantica[12], M. Maslov[3], V. Neverov[10], M. Romanelli[3], P. Siren[13], E.R. Solano[11], M. Stamp[3], T. Tala[13], M. Valisa[12], Valovic[3], D. Valcarcel[3], J. Varje[7], M. E. Viezzer[14], H. Weisen[15], S. Wiesen[2] and JET contributors[*]

Eurofusion Consortium JET, Culham Science Centre, Abingdon, UK,
[1]Instituto de Plasmas e Fusão Nuclear, IST, Universidade de Lisboa, Portugal, [2]Forschungszentrum Jülich GmbH, Germany, [3]CCFE, Culham Science Centre, Abingdon, UK , [4]Oak Ridge National Laboratory, Oak Ridge, USA, *[5]LPP-ERM/KMS, Brussels, Belgium, [6]IPP, MPG, Germany, [7]Aalto University, Finland, [8]PFSC, Boston, USA, [9]DRFC, CEA, France,[10] NRC Kurchatov, Russia,* [11]Laboratorio Nacional de Fusión, CIEMAT, 28040, Madrid, Spain*, [12]ENEA, Italy, [13] VTT, Finland, [14]University of Seville, Spain, [15]SPC-EPFL, Switzerland*

**See the author list of "Overview of the JET results in support to ITER" by X. Litaudon et al. to be published in Nuclear Fusion Special issue: overview and summary reports from the 26th Fusion Energy Conference (Kyoto, Japan, 17-22 October 2016)*

Abstract. The hydrogen campaign completed at JET in 2016 has demonstrated isotope ratio control in JET-ILW using gas puffing and pellets for fuelling, Neutral Beam Injection alone or in combination, with Dα/Hα spectroscopy as a diagnostic. The plasma properties such as confinement, L-H threshold, density limit depend on the isotope composition. The L-H transition power increases with the hydrogen concentration with a wide plateau in the range $0.2<n_H/(n_D+n_H)<0.8$. Energy confinement is significantly lower in hydrogen than in comparable deuterium ELMy H-mode plasmas, suggesting an isotope mass scaling that is stronger than in IPB98(y,2). In L-mode, the isotope dependence of confinement is weaker. The H-mode density limit in hydrogen is up to 35% lower than in heuterium, whilst it is found to be higher in L-mode. The lower ion mass leads to reduced tungsten sputtering in hydrogen plasmas. During the campaign, the $n_D/(n_D+n_H)$ ratio dropped to ~1% in only a few discharges after the last deliberate introduction of deuterium, although it was seen to rise again to ~2% with several seconds of exposure of the divertor tiles to ~10MW of auxiliary heating. Several ICRH scenarios were also tested in hydrogen plasmas.

1. Introduction

The dependence of plasma properties on the main ion isotope mass, as well as on isotope composition is relatively unexplored and has potentially a significant impact on the performance of future fusion devices. An experimental investigation of isotope and composition dependences is also likely to provide stringent tests for plasma transport models. Isotope experiments in the JET first deuterium-tritium campaign (DTE1) [1,2] in 1997 were relatively brief and were hampered by fairly crude diagnostics by current standards, especially concerning the resolution of the H-mode pedestal. The hydrogen (H) campaign completed at JET in 2016 is part of a planned multi-campaign effort including experiments in deuterium (D), H and tritium (T), leading up to experiments in D-T mixtures. Its aims are to explore the dependence of heat, particle, impurity and momentum transport and ELM behaviour in H, D and H-D mixtures, both in the plasma core and the pedestal. An important objective is to devise and test strategies for isotope ratio control for the future D-T campaign. Additional objectives include the isotope dependencies of the density limit, SOL transport, material

migration, retention and recycling of hydrogenic species and ICRH scenarios. Assessing the residual D concentration with near pure H operation was also an important goal, as it allows an estimate of the D-T neutron fluence in the future full T campaign, for which the neutron budget assumes $n_D/(n_D+n_T)=1\%$. NBI power in pure hydrogen was limited to 11MW while up to 7MW of ICRH were available.
We wish to stress that this manuscript was written within a few weeks of the end of the 2016 hydrogen campaign. Whilst we don't believe that there will be any major changes to the observations presented here, the data remain subject to revision.

2. Measuring and monitoring of the isotope ratio

The diagnostics for edge and vessel ratios included Hα/Dα spectroscopy in the divertor and main chamber [3], residual gas analysis [4] and a three-species Neutral Particle Analyser (NPA) set to a low energy range (5-40keV) for measuring D and H atom fluxes from the confined plasma near the LCFS [5]. After the last introduction of D by pellets into H plasmas, marked by an arrow in fig.1, no further D was injected until the last day of the campaign. The residual D concentration decreased to ~1%, as consistently measured using spectroscopy and residual gas analysis. NPA analysis using the lowest energy channel (5keV), which is least affected by the NBI slowing down distribution, and multi-shot averaging indicated residual thermal D levels down to between 0.5 and 1% using a simple model [6]. Background counts at energies between 20 and 40keV in the NBI slowing down distribution, showed that the residual D in the H beams was at most $\sim 10^{-3}$. Prolonged heating (several seconds at ~10MW) of the divertor tiles was seen to lead to a gradual increase of neutron rates and D content from ~1% to ~2%, which we interpret as due to outgassing of deuterium.

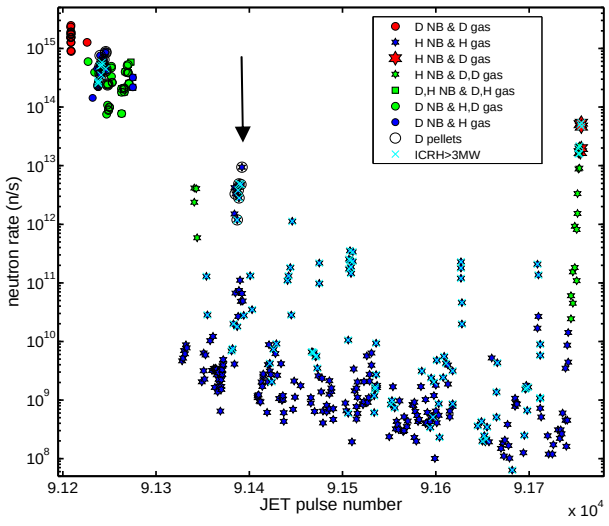

Fig1. Evolution of the neutron rates over the duration of the campaign and restricted to discharges with NBI power in the range 7-12MW. The symbols indicate different experiments. The arrow marks the last introduction of D before the last day of the campaign.

Isotope ratios for the plasma core were inferred with an accuracy of ~10% from the neutron rates, which were primarily from beam-thermal reactions in the presence of D NBI and from thermal-thermal reactions when no D NBI was used and no energetic ion tail was produced by ICRH. After the last introduction of D into the plasma, neutron rates dropped to $\sim 10^9 s^{-1}$ as compared to $\sim 2\times 10^{15}$ for comparable D plasmas heated by 10MW of D NBI (fig.1). These rates are consistent with those expected from thermal D-D reactions with $n_D/(n_D+n_H)\approx 1\%$.

3. Isotope ratio control in the mix H & D phase.

The H campaign allowed a test of strategies to control the D/T ratio in the future JET D-T campaign using gas puffing, NBI fuelling and pellets. Real time control of the isotope ratio with only H and D gas puffing and Hα/Dα spectroscopy as the diagnostic proved to be very

effective in both L- and H-mode plasmas allowing for controlled swings of the isotope ratio of several tens of % in only 2-3 seconds. Divertor and main chamber fuelling were similar in effect. The ideal scheme for achieving a constant isotope ratio profile was by setting both gas and NBI H and D fuelling rates to near the desired isotope ratio. Unfortunately H and D beams were available together only for a small number of discharges. However, even with NBI fuelling with only one species, good isotope ratio control was achieved. The core ratio in that case differed from the edge ratio by only 10-15%, roughly as expected from the effect of particle transport, assuming $D \approx \chi_{eff}$.

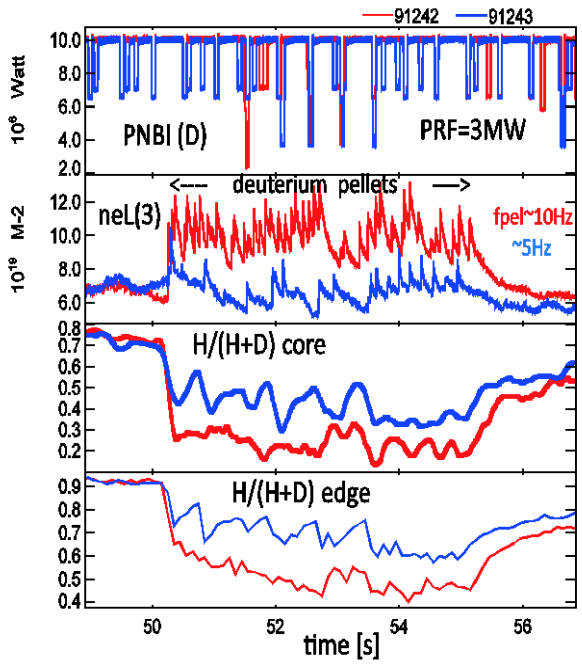

Fig 2. Core isotope ratio control using D pellets injected into a H majority H-mode plasma for two discharges. Top: NBI power, notched for improved CXS Ti measurements. 2nd box: line integrated density showing impact of pellets, 3rd: core isotope ratio inferred from neutron rates, bottom: edge isotope ratio from Hα/Dα spectroscopy

In ITER, two pellet injectors, one for D and one for T, are planned for controlling the isotope mix in the core [7]. In JET, we mimicked the ITER situation by injecting shallow D pellets into predominantly hydrogen plasmas, with the aim of establishing a core mix with 50% D. These 1.7T, 1.4MA H-mode plasmas were externally fuelled by H gas puffing and heated with ~10MW of H or D beams, as well as by ~3MW ICRH at the second harmonic hydrogen resonance (51MHz). The D pellets, 20-30mm^3 in size, were deposited in outer ¼ of the minor radius via a vertical launch track at the HFS (High Field Side). Fig. 2 shows two similar discharges with fuelling rates of 5 and 10Hz. It is seen that the target isotope ratio is approximately achieved with 5Hz pellets (blue traces). This fuelling rate is comparable to the underlying hydrogen gas fuelling rate. The case shown in fig. 2 is for D beams into H plasmas, allowing the best measurement of the core Deuteron density thanks to beam-plasma neutrons. No 4th harmonic D acceleration, whether beams are present or not, is predicted with 2nd harmonic by the TOMCAT code [8]. This was experimentally verified, eliminating the possibility that the core isotope ratio measurement based on the neutron rate could be affected by resonant acceleration of D.The experiment was repeated using pure hydrogen beams with a similar result, the core isotope ratio being inferred from thermal neutron rates. These experiments provide useful data for testing models used for the control of hydrogen isotopes in ITER using pellets and demonstrate that core hydrogen plasma can be fuelled using pellet injection.

4. L-H transition dependence on plasma isotope composition

The necessary power threshold to access H-mode has been studied in hydrogen and mixed hydrogen-deuterium mixtures, and compared to reference deuterium pulses. Fig. 3 shows the results for L-H transition power threshold as a function of line-averaged density for different isotope combinations and different heating schemes. The threshold is quantified as the total

auxiliary input power, plus Ohmic heating, minus the time derivative of the stored energy, minus charge exchange losses, minus an estimate of the radiated power in the core from bolometer chords. All data is at the same plasma current and magnetic field (1.7MA/1.8T), the same plasma shape with the outer strike point on the horizontal divertor target plate, which is the configuration with the lowest power threshold in JET-ILW. Several notable trends are observed, both for the value of P_{L-H} at fixed density and for variations of the minimum of the dependence of P_{L-H} on density. Considering only the pulses with dominant ICRH heating, the value of the power threshold in hydrogen plasmas is about 2-2.5 times larger than in deuterium, which is generally consistent with previous results [16]. The difference between hydrogen and deuterium is larger in the low density branch of the L-H transition than in the high density branch. Also, the value of the minimum of P_{L-H} as a function of density going from deuterium to hydrogen as shown in fig. 3. Future analysis will assess the relative partition of heating between electrons and ions in this data. We also find that for most densities, the threshold in 50/50 hydrogen/deuterium mixtures is equal to about the average of the threshold in pure hydrogen and deuterium plasmas (fig.4). The figure shows that a small admixture (<20%) of one species makes a large change to P_{L-H}.

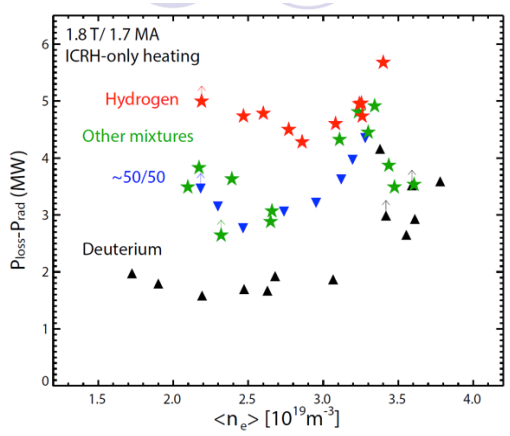

Fig 3: L-H transition power threshold for plasmas with concentration ratio H/(H+D)<0.1 (black), 0.4< H/(H+D)<0.6 (blue), and H/(H+D)>0.9 (red).

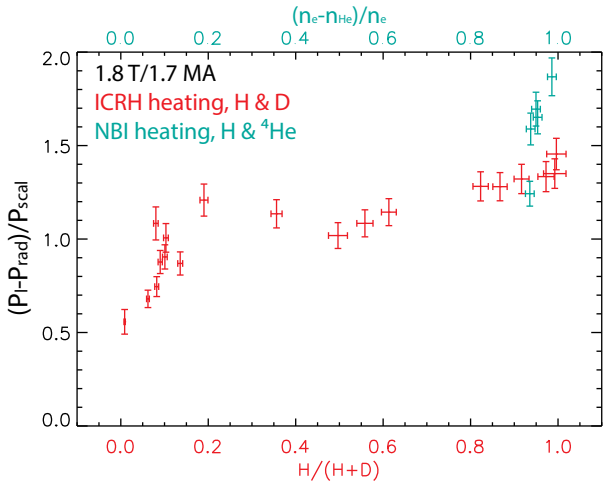

Fig 4: L-H transition power threshold for varying H/D (red) and H/He4 (green) ratio.

The L-H transition studies have also revealed an n=0, m=1 magnetic oscillation, starting immediately at the L to H transition (so-called M-mode at JET) [9]. While the magnetic oscillation is present, a weak ELM-less H-mode regime is obtained with a clear increase of density and a weak electron temperature pedestal. The axisymmetric magnetic oscillation is dominantly up-down, and its typical frequency is ~ 1 kHz. The frequency appears to scale with the poloidal Alfvén frequency. The mass dependency was confirmed by the comparison of H and D ICRH heated plasmas and the density and current dependencies were studied in deuterium. Pedestal and SOL diagnostics show that the oscillation is localised at the pedestal, and the mode modulates particle and heat fluxes to the target.

5. Energy confinement dependence on plasma isotope composition

The energy confinement in hydrogen plasmas was compared to previously produced deuterium reference sets achieved under similar conditions. Fig. 5 shows the stored energy as function of total heating power for the two species in discharges with B_T=1.7T, I_p=1.4MA. Confinement in hydrogen plasmas is lower than in deuterium, as already reported from JT-

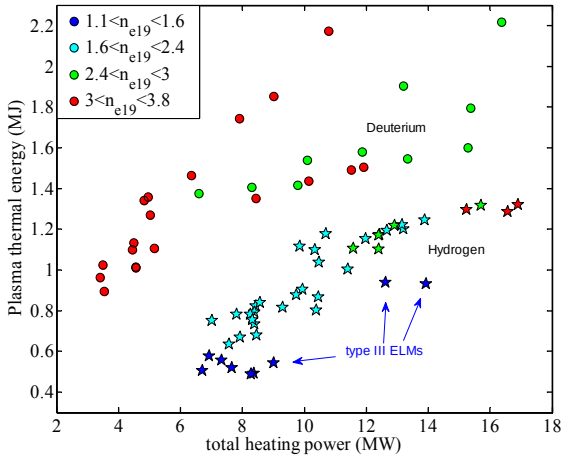

Fig.5 Plasma stored energy from Thomson scattering, assuming T_i=T_e in H (✶) and D (●) H-modes at 1.7T, 1.4MA. Symbols refer to volume average density.

60U [10]. This is in part due to the difficulty (not observed in JT-60U [10]) of achieving similar densities in both deuterium and hydrogen plasmas. Unlike in deuterium H-modes, for which there is little or no margin to influence the density by gas puffing, the density in hydrogen H-modes can be increased although requiring very high gas puffing to achieve the same densities as the deuterium references; these were only achieved in a few cases. Another difficulty was that due to the high L-H threshold in hydrogen, even at high power (10MW and more) type I ELMy H-modes with marginal performance or type III ELMy H-modes were obtained at 1.7T.

Preliminary power law scalings in type I ELMy H-mode indicate an atomic mass scaling for ELMy H-modes significantly stronger than in IPB98, but this dependence remains subject to revision as further data become available (e.g. T_i). Mixed H-D H-mode plasmas exhibit confinement properties intermediate to those of pure D and pure H plasmas. L-mode data analysed so far are in stark contrast with H-mode data, as the confinement was found to depend only weakly on the isotope species.

6. ICRH scenarios in hydrogen and mixed isotope plasmas

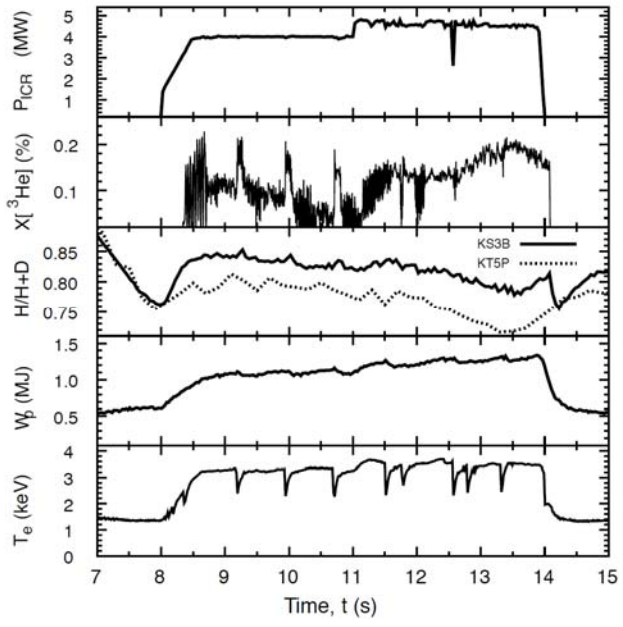

Fig.6 ICRH three-ion heating scenario (#91012, 3.1T, 1.8MA), from top to bottom: ICRH power, ^{3}He concentration, isotope ratio from spectroscopy (-) and residual gas analysis (…), plasma stored energy W_p, (e) central plasma electron temperature from ECE.

Several ICRH scenarios were tested in majority H plasmas, with applications to JET D-T experiments and the ITER non-active phase. These included successful demonstrations of the efficacy of the three-ion D-(^{3}He)-H and the Doppler shifted D-(D_{NBI})-H scheme, the classical ^{3}He minority scheme and 2nd harmonic H heating. The three-ion ICRH scheme is a new and potentially important scheme suitable for mixed species plasmas with proposed applications to the next JET DT (DTE2) campaign and to ITER. In this scheme, the mode conversion layer established by the two main species is arranged, by a suitable choice of the isotope ratio, to be close to the fundamental cyclotron frequency of the third (minority) species, which efficiently absorbs the power thanks to the large amplitude left hand polarised wave component [11]. Effective plasma heating with trace amounts of ^{3}He ions (~0.2%) and an edge isotope ratio H/(H+D) ≈ 0.80

plasmas has been demonstrated with ICRH as the only auxiliary heating method (fig.6). The observed sawtooth stabilisation and the detection of gamma rays and neutrons from ^{3}He-^{9}Be reactions confirm that the ICRH caused ^{3}He acceleration. These experiments have established the D-(^{3}He)-H scenario as an efficient tool for plasma heating and energetic ion generation, paving the way for applications in D-T plasmas using the T-(^{9}Be)-D and possibly the T-(^{7}Li)-D schemes. As a part of three-ion scenario development, the idea of using D-NBI ions as the third ion species resonating in the vicinity of the mode conversion layer by virtue of the Doppler shift ($k_{//}v_{//}$) has also been tested. This synergetic NBI+RF 3-ion scenario resulted in a significant enhancement in neutron rate (more than by a factor of 10) with energetic neutrons and gamma-ray emission associated with energetic D ions.

The classical ^{3}He minority and the 2nd harmonic fundamental ICRH scenarios proved to be robust in hydrogen plasmas with efficiencies of $\eta\sim60\%$, indicated by preliminary analysis using the break-in-slope method. Classical ^{3}He minority heating close to its fundamental cyclotron frequency (f=33MHz at B_T=3.15T) provided minority heating at modest concentrations (~2%) and electron heating at ~4%. The low background neutron rates in near pure H plasmas (~$10^{9}s^{-1}$) allowed the observation of nuclear reactions involving energetic ^{3}He, chiefly ^{3}He+^{9}Be$\rightarrow^{11}$C+n [12], which raised the neutron rates by up to 3 orders of magnitude, as marked with magenta x signs in fig.1. Second harmonic H majority heating at low field ($B_T\approx1.7$T for f=51MHz) was also used extensively for plasma heating in the experiments described above, both in hydrogen and mixed plasmas (marked as cyan x in fig.1). At low density and in the presence of H-NBI, this scenario lead to an enhancement of the neutron rates from ~10^{9}n/s to as much as 2×10^{12}n/s in some cases, providing evidence for the creation of fast deuterons by reactions of ICRH-accelerated protons with energies up to ~1MeV with Be ions present as intrinsic impurities via the p+^{9}Be$\rightarrow$2 4He+D reaction and subsequent neutron production from the D+D$\rightarrow^{3}$He+n reaction [13].

Fundamental Deuterium minority heating was tested with ICRH alone (B_T=3.2T, f=25MHz), with an efficiency of $\eta\sim40\%$ from break-in-slope analysis. Hydrogen fundamental ICRH was found to be a poor heating scheme with $\eta\sim20\%$, even if NBI is available to ensure preheating (f=51MHz, B_T =3.3T).

7. L- and H-mode density limit in hydrogen

Tokamak operation at high density with a partially or fully detached divertor is considered as the baseline scenario for ITER and future fusion power plants. The establishment of a detached divertor at densities close to the Greenwald limit n_{GW} (density limit, DL) is mandatory for both maximising the fusion power and reducing the heat loads on plasma-facing components, in particular onto the divertor target plates. Substantial efforts from JET and AUG have been made to identify the underlying mechanisms via developing scaling laws [14, 15] responsible for the H-L transition at high density in metallic machines. Previous experimental studies in JET-C in L-mode [16] and H-mode [17] showed that different isotopes lead to a different behaviour of the density limit. In order to investigate this latter issue, L- and H-mode density limit experiments were performed in H plasmas and compared with the results obtained in D plasmas.

In L-mode, the density limit is defined as the plasma density prior to the so-called “density limit” disruption, whilst in H-mode, the density limit is defined as the density at which the H to L transition occurs. The experimental results show apparent differences for the DL in L-mode and H-mode plasmas: (1) in L-mode density limit is up to 10% higher in hydrogen than in deuterium plasmas (fig. 7a) whilst in H-mode, the DL is up to 35% lower in hydrogen than in the deuterium plasmas. (2) In L-mode plasma the divertor plasma configuration has a modest impact on the DL, reducing the difference in DL density between H and D from 10%

in vertical configurations to 5% in horizontal configurations. The detachment onset density, i.e., the density at which ion current to the target plate saturates, is 30% higher in H than in D. EDGE2D-EIRENE simulations predict up to 50% higher divertor densities in D than in H, identifying the divertor density as the root cause for the difference in the DL in H and D plasmas [18]. (3) In H-mode, the density limit is not related to an inward collapse of the core plasma induced by the overcooling of the plasma periphery by radiation. Both in H and D plasmas, the total radiation and the bulk radiation stays almost constant throughout the entire pulse, from ELMy H-mode to L-mode. (4) The H-L transition in both D- and H-plasmas is correlated with neither detachment nor the X-point MARFE, thus these are not limiting the plasma density. (5) The density limit in H-mode on JET-ILW is nearly independent of power, whilst in L-mode, a 20% increase is observed on the rollover density dependence with power in the range used in these experiments for D- and H-plasmas. The measured Greenwald fractions in this experiment, which was in the vertical divertor target configuration, are found to be consistent with the predictions from a theoretical model based on MHD instability theory [19] in the near-SOL as shown in fig. 7b.

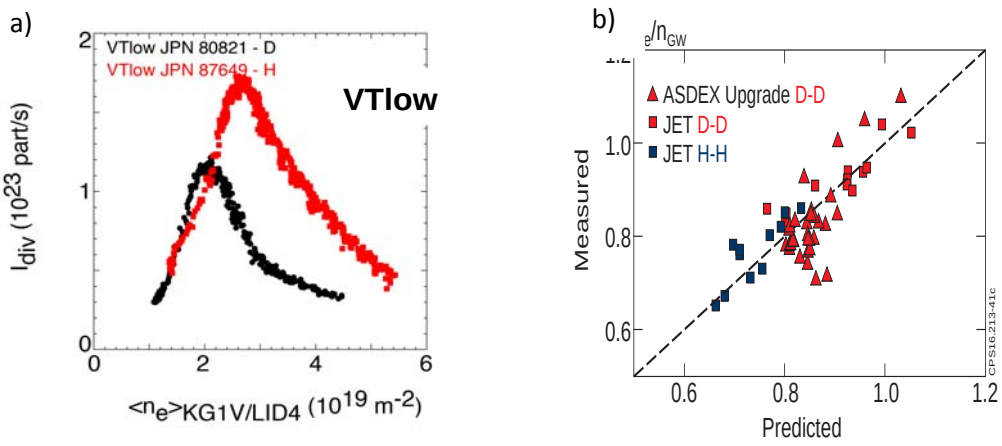

Figure 7: (a) Ion current saturation at the divertor for two similar plasmas in H (red) and in D (black). (b) Experimental measurements of the Greenwald, in gas fuelled H-Mode DL discharges in JET-ILW (vertical target configuration) and AUG tokamaks, plotted against the predicted Greenwald fraction from the Goldston model.

8. Tungsten sources in Hydrogen plasmas

L-mode and inter-ELM W sources in JET-ILW are determined in pure deuterium discharges by Be ions impinging on the W divertor [20]. Detailed studies revealed that Be^{2+} ions are the dominating species with a maximum concentration of 1% with respect to the deuterons. Also, the corresponding physical sputtering threshold has been measured and the absence of the W source at impact energies below 35eV at the outer target plate measured. As expected, a similar observation with an energetic threshold was made in hydrogenic plasmas as depicted in figure 8 showing the effective W sputtering yield related to the hydrogen recycling flux as proxy for the impinging ion flux at the target plate. However, the source strength is reduced as the cause of the W sputtering, the Be ion influx is reduced too. This is due to the fact that primary source of the Be, erosion at the main chamber by physical sputtering [21] by protons is lower than by deuterons due to the change in mass. As a consequence, the inter-ELM and L-mode W source in hydrogen plasmas are significant lower than in deuterium, which allow safe operation at lower plasma fuelling rates before critical W core concentrations or W

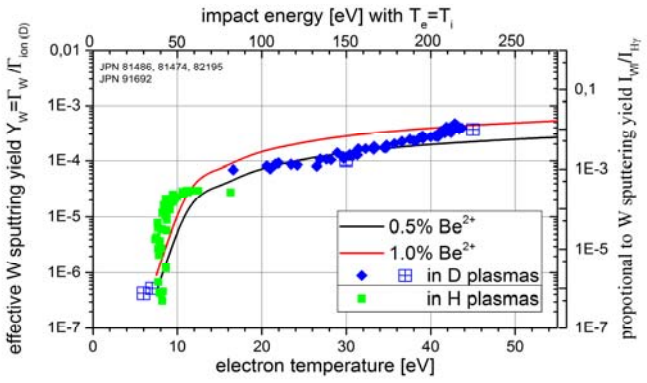

Fig. 8 Effective W sputtering yield at the energetic threshold around 35 eV assuming T_e=T_i and T_e at the threshold of 8eV.

accumulation sets in. The impact of the isotope exchange is even more pronounced during the ELM impact, as in this case the flux of hydrogenic ions is predominantly responsible for the W source [22]. The difference in the mass of the projectile is determining the total strength of the ELM-induced W-source in hydrogen and deuterium plasmas as predicted by binary-collision approximation calculations and predicted by [20]. This also widens the operational window at low fuelling rate in hydrogen plasmas in comparison to deuterium plasmas.

9. Outlook

Whilst many of the results of the 2016 hydrogen campaign are still subject to revision and need further analyses, the success of the campaign bodes well for the multi-campaign effort (which will include experiments in full T and in D-T), of investigating isotope effects in conditions close to those expected in ITER. Further analysis, in particular, will focus on detailed understanding of the SOL and pedestal behaviour for different isotopes and how they determine global transport properties, H-mode access and density limits.

10. References

[1] G. Saibene et al, Nucl. Fusion **39** (1999) 1133
[2] J G Cordey et al, PPCF **42** (2000) A127
[3] V.S. Neverov et al, submitted to Nuclear Fusion 2016
[4] U. Kruezi et al, Rev.Sci. Instrum. **83** (2012) 10D728
[5] V.I. Afnasyev et al. Rev. Sci. Instrum. **74** (2003) 2338
[6] K. Günther et al. Journal of Nuclear Materials **241-243** (1997) 462
[7] Maruyama S. *et al* 2012 *Proc.24th Int. Conf. on Fusion Energy (San Diego, 2012)* ITR/P5-24
[8] D. Van Eester and R. Koch, Plasma Phys. Control. Fusion **40** (1998) 1949
[9] E. R. Solano et al, accepted for publication in Nucl. Fusion
[10] H. Urano et al, Nucl. Fusion **52** (2012) 114021
[11] Y. Kazakov et al, Nucl. Fusion **55** (2015) 032001
[12] M. Gatu Johnson et al, Nucl. Fusion **50** (2010) 045005
[13] A. Krasilnikov et al, IAEA FEC, 2016, Kyoto (post-deadline)
[14] A. Huber et al., Journal of Nuclear Materials **463** (2015) 445–449
[15] A. Huber et al, Nucl. Mater. Energy, submitted.
[16] C. Maggi et al, Nuclear Fusion, Vol. **39**, No. 8 (1999) 979
[17] K. Borrass et al, Contrib. Plasma Phys. **38** (1998) 130–135.
[18] J. Uljanovs et al, Nucl. Mater. Energy, submitted.
[19] R. J. Goldston, Journal of Nuclear Materials **463** (2015) 397–400
[20] S. Brezinsek et al, J. Nucl. Mater **463** (2015) 11
[21] S. Brezinsek et al, Nucl. Fusion **54** (2014) 103001
[22] Ch. Guillemaut et al, PPCF **57** (2015) 85006

Acknowledgement: This work was carried out within the framework of the EUROfusion Consortium and received funding from the EURATOM research and training programme 2014-2018 under grant agreement No 633053. The views and opinions expressed herein do not necessarily reflect those of the European Commission.